

Coordinating Power Grid Frequency Regulation Service with Data Center Load Flexibility

Ali Jahanshahi

University of California, Riverside
Riverside, CA, USA
ajaha004@ucr.edu

Sara Rashidi Golrouye

University of California, Riverside
Riverside, CA, USA
srash034@ucr.edu

Osten Anderson

University of California, Riverside
Riverside, CA, USA
oande001@ucr.edu

Nanpeng Yu

University of California, Riverside
Riverside, CA, USA
nyu@ece.ucr.edu

Daniel Wong

University of California, Riverside
Riverside, CA, USA
danwong@ucr.edu

Abstract

AI/ML data center growth have led to higher energy consumption and carbon emissions. The shift to renewable energy and growing data center energy demands can destabilize the power grid. Power grids rely on *frequency regulation reserves*, typically fossil-fueled power plants, to stabilize and balance the supply and demand of electricity. This paper sheds light on the hidden carbon emissions of frequency regulation service. Our work explores how modern GPU data centers can coordinate with power grids to reduce the need for fossil-fueled frequency regulation reserves. We first introduce a novel metric, *Exogenous Carbon*, to quantify grid-side carbon emission reductions resulting from data center participation in regulation service. We additionally introduce *EcoCenter*, a framework to maximize the amount of frequency regulation provision that GPU data centers can provide, and thus, reduce the amount of frequency regulation reserves necessary. We demonstrate that data center participation in frequency regulation can result in Exogenous carbon savings that oftentimes outweigh Operational carbon emissions.

1 Introduction

Data centers are essential infrastructures for supporting cloud services and modern ML/AI workloads. Data centers are now one of the leading electricity consumers worldwide. In the United States, data centers accounted for $\sim 4\%$ of electricity consumption in 2024, and as high as 9.1% by 2030 [1]. For some states, such as Virginia, data centers account for 25% of the state's total electricity consumption, with this projected to grow to 46% by 2030 [1]. This rising electricity demand increases carbon emissions. By 2030, global greenhouse gas emissions from data centers will be equivalent to 40% of total US greenhouse gas emission [2]. This intensifying environmental impact has led industry leaders to prioritize reducing the carbon footprint of data centers. For instance, Google and Microsoft are committed to powering data centers with only carbon-free energy by 2030 [3, 4].

Carbon footprint includes *Operational Carbon* emissions, such as electricity consumption, and *Embodied Carbon* emissions, such as supply chain activities. A major effort to reduce operational carbon is to shift towards renewable energy sources. Despite investments in renewable energy—an increase from 12% to 31% in carbon-free generation [5]—cloud providers continue to face a mismatch between

their substantial data center demand and the available renewable energy supply.

However, both AI/ML data centers and renewable energy sources can cause instability to the power grid's frequency [6, 7]. Power system operators need to dynamically balance energy generation and energy consumption to maintain grid stability through *frequency regulation services*, where *frequency regulation reserves* are expected to adjust their power levels based on 2-second granularity *frequency regulation signals*. Since the intermittent nature of renewable energy sources cannot adjust output quickly enough to balance the grid, power grids still rely on fossil fuel-based power plants as a frequency regulation reserve.

Both AI/ML data centers and *renewable energy sources* increase the demand for frequency regulation reserves. Insufficient frequency regulation reserves can (1) impede the growth of future AI/ML data centers or (2) cause the power grid to intentionally reduce the amount of renewable energy available in the grid, leading to worse carbon emissions. ***This paper aims to shed light on the hidden carbon emissions cost of power grid frequency regulation reserves, and how data centers providing frequency regulation service can help lower this.*** Since data centers can account for a large fraction of total grid energy consumption, the power flexibility of data centers hold a large potential for reducing the demand for traditional frequency regulation reserves to (1) support the growth of future AI/ML data centers and (2) enable greater renewable energy penetration. Towards this goal, this paper makes the following main contributions:

Contribution 1: We propose *Exogenous Carbon*, a new metric that quantifies the grid-side carbon emission reduction due to data center frequency regulation services. Data center regulation service can reduce the demand of traditional frequency regulation reserves, thus, lowering the carbon emissions of the power grid. To the best of our knowledge, *our work is the first to quantify the grid-side carbon emissions benefits of data center participation in frequency regulation*.

Contribution 2: We propose *EcoCenter*, a framework to maximize *frequency regulation provision*, and thus, exogenous carbon savings of AI/ML GPU-based data centers. While prior approaches [6, 8] demonstrated data center regulation service by modulating CPU power, GPUs provide greater power flexibility opportunity (5x of CPU) and GPU power knobs present unique challenges. Frequency regulation service is challenging due to fine-grain 2-second power

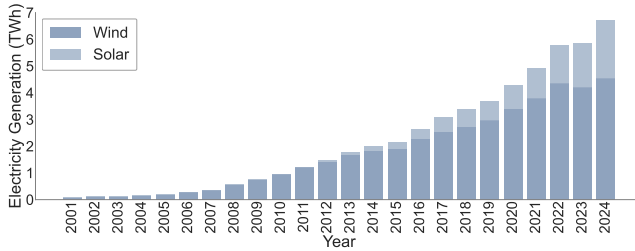


Figure 1: The growth of renewable solar and wind energy in the US [5] and its intermittent nature is increasingly destabilizing electrical power grids [19].

modulation requirements and the limitations of GPU power management knobs [9], such as limited accuracy and limited usable dynamic power range due to high active idle power. EcoCENTER overcomes this by carefully coordinating power capping, core allocation, and multi-GPU coordination of co-located workloads.

2 Background

2.1 Carbon Emission Trends

In Data Centers. Recent hyperscale data centers consumes upwards of 100 MW [10]. Globally, data center electricity is expected to increase by 160% by 2030, with data centers consuming 3-4% of worldwide electricity [11]. Training and deploying machine learning models also contributes significant carbon emissions. For example, training the LLaMA2-70B language model produced 291.42 tons of CO₂ equivalent, despite state-of-the-art efficiency techniques [12].

Recently, carbon-aware data center management techniques have been proposed to reduce the carbon footprint of ML workloads. For example, placing carbon-aware data centers in regions with greener energy sources [13]. Similarly, intelligent scheduling and coordination between data center operators and power grids can align flexible data center workloads with periods or regions of high renewable availability (i.e., low carbon intensity) [14–18]. However, further integration between data centers and power grids are needed to reduce the carbon footprint of machine learning workloads.

In Power Grids. The need to reduce greenhouse gas emissions has made sustainable power grids a priority worldwide. In the United States, the integration of renewable energy sources, like solar and wind, increased by 54.5% from 2018 to 2024, representing growth of more than half over these 6 years, as shown in Figure 1. Due to the intermittent nature of renewable energy sources, this rapid integration poses significant challenges for grid stability to balance both electricity supply and demand [6, 7], requiring power grids to rely on demand response services to provide grid reliability.

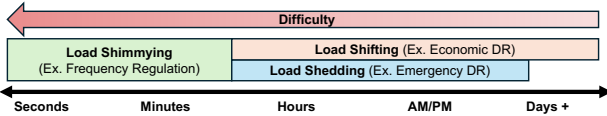


Figure 2: Various types of demand response (DR) services work across different timescales. Our work targets frequency regulation service, the most challenging DR service.

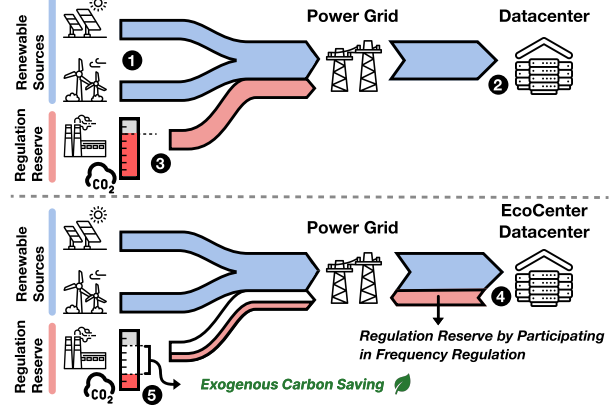


Figure 3: Power grids must balance 1 the power generation of renewable resources and 2 end-user power consumption by relying on 3 fossil-fuel power plants for regulation reserves. This work explores 4 how data centers can contribute to grid balancing to reduce reliance on traditional regulation reserves and quantify the grid-side carbon footprint benefits 5.

2.2 Demand Response Services

Electricity market services provided by loads, such as datacenters, are *demand response* (DR) services which relies on electricity consumers to adjust their load following a signal from the power utility. As shown in Figure 2, DR services can be broadly classified into three categories: Load Shifting, Load Shedding, and Load Shimmying [20].

Many prior works have explored data center participation in emergency demand response, a type of Load Shedding service operating over hours, which require data centers to reduce load during power grid emergencies [7, 14, 21–23]. Data centers shifting workloads to run during periods of greater renewable energy generation or cheaper electricity price are examples of Load Shifting service [15–17, 24–31].

The most challenging DR service is Load Shimmying, which requires participants to vary their load in minute or even second granularity. Examples include Load Following service that operates at 5-minute granularity, or advanced fast frequency regulation service, that operate at 2-second granularity (which this work targets).

2.3 Introduction to Frequency Regulation Service

To maintain electrical grid stability, operating frequency must be kept between 58.98Hz and 60.02Hz in the United States. As illustrated in Figure 3, the power grid must maintain a balance between renewable energy generation 1 and power consumption 2. However, the intermittent nature of renewable energy sources, like wind and solar, causes significant variation in power generation 1. These sources cannot adjust output quickly enough to balance consumption. Traditionally, grid balancing is achieved by adjusting *regulation reserve* generator output, typically by fossil fuel-based power plants, to match electricity consumption 3. Specifically, these *regulation reserves* can contribute a significant amount

of carbon emissions that is not accounted for in traditional carbon intensity metrics of power generation sources [32, 33]. In Section 3, we will discuss this limitation further.

Frequency Regulation Markets: Power system operators offer *frequency regulation services* in *day-ahead* or *real-time* markets. There are several Independent System Operators (ISO) that coordinates the movement of electricity through all or parts of regions in the USA. For example, PJM covers the eastern US and California ISO (CAISO) covers California. In this paper, we utilize the CAISO real-time market, which allows bids every hour at 60-minute granularity. Resources, such as data centers, submit into the market every hour their estimated energy consumption baseline (P_{avg}) and frequency regulation service provision capability (R), which represents the amount of power capacity (in MW) that the data center can commit to help balance the grid.

Regulation Signal: Frequency regulation service resources, such as data centers, modulate their power consumption to follow a *frequency regulation signal* ($r(t)$), which ranges from $[-1, 1]$ and is broadcast every 2 seconds by the ISO. ISOs ensure that the difference between two consecutive values of $r(t)$ does not exceed 0.5% of R [34].

Quantifying Quality of Frequency Regulation Service Provision: The revenue from frequency regulation service is also dependent on the *quality* of the service provided. This quality is quantified by a *performance score* [34], which is the average of delay, accuracy, and precision metrics. The performance score is calculated every 15 minutes by the ISO for each regulation resource [35]. ISOs typically certify a resource for regulation service provision after the resource achieving a performance score of 75% or better on three consecutive tests [34]. To maintain certification, resources must keep a performance score of 40% or higher, or be removed as a regulation resource.

Reward Pricing and Electricity Cost: Besides the electrical cost of the data center's electricity consumption, data centers also receive monetary rewards for participating in frequency regulation markets. By setting the energy consumption baseline (P_{avg}) and the amount of frequency regulation provision (R), data centers maintain power consumption at $P_{avg} + r(t) \cdot R$. The energy charge at time t equals the product of P_{avg} and the locational marginal price of energy. The revenue from providing frequency regulation service equals the product of R , the quality of the provided regulation service, and the frequency regulation service price.

2.4 Opportunities for Data Center Regulation Service

With data centers projected to grow to 3-4% by the end of the decade [11] and accounting for up to 46% of certain US state's electricity consumption [1], data centers can potentially provide a significant portion of frequency regulation capacity ④, reducing the reliance on fossil fuel power plants ⑤. Many prior works have explored the potential of data center participation in electricity markets [6, 8, 21, 22, 36–38]. However, many of these prior studies were limited to analytical studies or simulation, participated in slower demand response services (compared to fast frequency regulation) or targeted data centers running best-effort workloads, which limits the applicability in real-world scenarios. Most relevant,

PowerMorph [6] explore how data centers running *latency critical* workloads can participate in frequency regulation. However, PowerMorph only explore the economic benefits of frequency regulation and only modulates CPU power, an increasingly small fraction of AI/ML data center power consumption [39].

3 Quantifying Grid-side Carbon Impact of Data Center Regulation Service

In this section, we introduce how to quantify the grid-side carbon impact of data center frequency regulation and detail how data centers interact with power grids to impact this.

Data Center Emissions Modeling. Data center carbon emission (C_{DC}) is defined as the combination of *operational* carbon (C_{op}) and *embodied* carbon (C_{em}), $C_{DC} = C_{op} + C_{em}$.

Embodied carbon accounts for the carbon footprint when building the data center and manufacturing the data center components. Following methodologies from prior work [40], we derive *embodied carbon* from the aggregated manufacturing carbon footprint of the data center's hardware.

Operational carbon is the emissions produced from running a data center's day-to-day operations. This is typically based on the data center's energy consumption (E_{DC}) and the carbon intensity (CI_{gen}) of the power grid during data center operation, $C_{op} = E_{DC} \times CI_{gen}$ [13, 18, 41, 42].

Carbon intensity metrics are provided by power grid operators and measures the *average carbon emission* of the grid [43, 44]. The carbon intensity (CI_{gen}) is computed as $CI_{gen} = \frac{C_{gen}}{E_{gen}}$, where C_{gen} is the emissions from all energy generation sources and E_{gen} is the amount of all energy generation. Carbon intensity is usually measured in units of $gCO2eq/kWh$ and vary significantly based on the electricity mix and location [45].

Limitations of Data Center Emissions Modeling. Note that the carbon intensity metric provided by power grids only account for *power generation* and not *regulation reserves* [32, 33], which we will explain in the next subsection and Fig. 4. Therefore, the extent of existing carbon-aware data center interaction with power grids is to (1) reduce the data center's energy consumption (E_{DC}), which reduces grid-side carbon emissions from power generation, or (2) schedule/relocate workloads to a different time/location with lower carbon intensity (CI_{gen}). Clearly, existing modeling methodologies do not capture the emissions of grid-side regulation reserves, limiting the data center's ability to impact grid-side emissions.

3.1 Accounting For Hidden Emissions of Regulation Reserves

Figure 4 illustrates the interactions between grid frequency regulation reserves, data centers, and the "hidden" carbon emission factors that are currently unaccounted for in grid-reported carbon intensity metrics. This illustrative example has four 100MW data centers and four natural gas power plant with a minimum load¹ of 50 MW and a peak load of 100MW. In both scenarios, the grid is generating 300 MW of electricity with ± 100 MW of available regulation reserves.

¹Fossil-fuel power plants have a minimum stable operating load requirement in order to output power [46–48].

H1 Hidden emissions 1: Providing regulation service does not directly produce emissions. Each power plant provides $\pm 25\text{MW}$ of regulation reserve. This reserve is only used when the grid requires balancing, thus, *providing* reserves does not produce emissions, unless it *performs* regulation. This is the fundamental reason why grid-reported carbon intensity cannot directly incorporate the emissions of regulation reserves. Furthermore, performing regulation require power plants to both *increase* and *decrease* output compared to nominal levels, which add challenges towards tabulating regulation emissions.

H2 Hidden emissions 2: Power plants run at lower efficiency to provide regulation service. To provide $\pm 25\text{MW}$ of regulation reserve, the power plants operate at 75MW to provide 25MW of frequency regulation up and 25MW of frequency regulation down service. Power plants operate most efficiently at peak output [49]. Due to providing regulation, this power plant now operates at a less efficient output level of 75MW , which produce more emissions per MW of output.

H3 Hidden emissions 3: Providing regulation service may require more power plants. When data centers leverage workload flexibility to provide $\pm 25\text{MW}$ of regulation, it removes the grid-side carbon of performing regulation with fossil-fueled power plants and also allows power plants to operate more efficiently at 100MW output level. This also enable the dispatch of fewer power plants (3 instead of 4) in the grid to meet electricity demands. Therefore, data center participation in regulation service can have an out-sized carbon emissions benefit beyond the substituted regulation reserve.

3.1.1 Capturing Regulation Reserve Emissions. To capture these hidden emissions factors of regulation reserves, we extend operational carbon to include the impact of data centers on grid-side carbon emissions as following:

$$C_{op_{w/RS}} = E_{DC} \times CI_{gen} - \underbrace{(R_{DC} \times MER_{resv})}_{\text{Exogenous carbon, } C_{\text{exogenous}}} \quad (1)$$

, where R_{DC} is the amount of regulation provision provided by the data center and MCE_{resv} is the *marginal carbon emission* [41] of regulation reserves, which is the change in grid-side carbon emissions due to a change in regulation reserves in the grid. We call this new term *exogenous carbon*², $C_{\text{exogenous}}$, which collectively quantify the *grid-side* carbon emission impact of data center participation in frequency regulation services. With this term, **data centers now have an additional knob for carbon-impact by maximizing the amount of regulation provision, R_{DC}** .

The next challenge is in how MCE_{resv} can capture the aforementioned hidden emissions of regulation reserves. A simple model would be to only account for the carbon intensity of the power plant used for regulation, where $MCE_{resv} = CI_{resv}$. However, this would not fully capture the power grid dynamics of aforementioned “hidden emissions”, resulting in under-estimation of exogenous carbon impact.

Since marginal carbon emission captures the *change* in grid-side emissions due to a *change* in regulation reserves, we require

²Exogenous is defined as “relating to or developing from external factors”, hence, exogenous carbon relates to the various hidden carbon emission factors external to existing grid carbon intensity metrics.

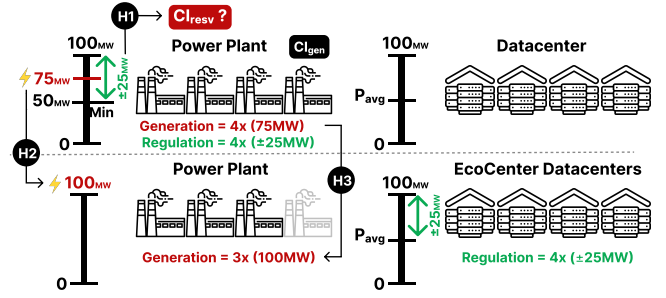


Figure 4: The “hidden emissions” of grid regulation reserves includes H1 unaccounted emissions of performing regulation service (grid only reports CI of generation), H2 regulation reserves cause power plants to run at lower efficiency, and H3 requires more grid resources to provide regulation capacity. Data center regulation service helps alleviate these emissions.

knowing the conditions of the grid with and without data center regulation service. Capturing all hidden emissions factor require a detailed power grid model that captures the emissions of *performing* regulation service and the power plants dispatched (along with output levels) to provide electricity generation and regulation reserves. In electricity markets, these are achieved through a *unit commitment* process.

3.1.2 Obtaining MCE_{resv} with Grid-side Unit Commitment Modeling. The unit commitment problem in electricity markets is the process of determining which power generation units should be turned on/off to meet expected electricity demand, at the lowest cost, while satisfying technical and operational constraints. It involves scheduling generators over a 24 hour period to ensure a reliable and cost-efficient supply of electricity. For example, CAISO performs unit commitment in a day-ahead market to schedule generation for the next day. Adding data center regulation reserves would have a notable impact to unit commitment in scheduling grid resources.

We formulate and solve the unit commitment problem as laid out in Anderson [50], which models CAISO and the Western Interconnection grid, totaling 14GW. We assume that 770MW of frequency regulation must be held at all times, which is 5.5% of grid capacity for regulation provision. From historical electricity pricing and demand traces (circa 2022), the model solves at hourly granularity the generation unit commitment requirements to meet electricity demands and regulation reserves. Similar high-fidelity power grid simulation model is used by the California Public Utility Commission and California Independent System Operators, demonstrating its utility in power systems planning.

Using this model, we can identify the “hidden” cost of regulation reserves by first running the model with regulation reserves provided by traditional generation sources to obtain the total carbon emissions of the grid. Then we run the model with data center regulation service to obtain the total carbon emissions of the grid with datacenter regulation service. The difference of both values provides the “hidden” grid-side carbon emission impact of data center frequency regulation, which we use to obtain the grid-detailed marginal carbon emission, MCE_{resv} , for use in Eq. 1.

4 EcoCenter Framework

We now introduce EcoCENTER, a framework for GPU data centers to maximize the amount of regulation provision (R_{DC}) and maximize benefits to grid-side exogenous carbon savings. Unlike prior works that minimizes **datacenter-side** power *consumption* to save *operational* carbon, our work shows that you can maximize **datacenter-side** power *modulation* to save **grid-side** emissions of regulation reserves, which data centers account for with the exogenous carbon term in Equation 1.

EcoCENTER focuses on GPU data centers due to GPUs now dominating power consumption in data centers [39], consuming 5x more than CPU power and thus providing the greatest source of workload flexibility and potential for regulation reserve provision. GPU TDP has grown significantly with each new generation, going from 300W (P100) \rightarrow 400W (V100) \rightarrow 700W (H100) \rightarrow 1000W (B200) over the last decade [12, 51–53].

GPU challenges: Compared to prior CPU-based data center regulation service [6, 8], GPUs power modulation present unique challenges compared to CPUs. (1) CPUs provide significant low-power states optimized for low utilization that enable >80% of dynamic power range to be accurately modulated. Thus, CPU-based policies do not directly translate to GPUs. (2) Without a focus on low utilization low-power states, GPUs consume significant active idle power, resulting <50% of dynamic power range available for modulation. (3) GPU power management has limited low-power states, leading to limited accuracy [9].

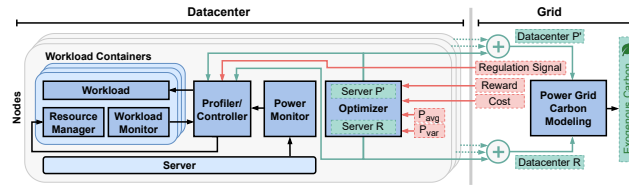


Figure 5: EcoCENTER overview. Red boxes show the inputs to the framework and the green boxes show the output.

4.1 System Overview

EcoCENTER overcomes GPU’s power modulation limitations by coordinating GPU DVFS, compute unit scaling, and multi-GPU load assignment as novel power modulation knobs. Figure 5 illustrates a high-level overview of EcoCENTER. In our demonstration, EcoCENTER is designed to integrate seamlessly into containerized (Docker) data center environments, but can be generalized to other deployment styles.

Data center-side: On each server, a *Controller* is deployed that reshapes the power consumption of servers running GPU workloads to adhere to the *regulation signal* issued by the grid, alongside the average power of the server for the next hour (Server P) and regulation provision the server is providing (Server R), which are determined by the *Optimizer*. The *Optimizer* decides the amount of regulation provision (Server R) by each server based on the predicted average load (P_{avg}) of the server and its variance (P_{var}). We predict average load for the next hour based on historical load patterns [54–60].

Power grid-side: The grid provides the *electricity cost* and *regulation reward* to the data center and asks the data center to modulate

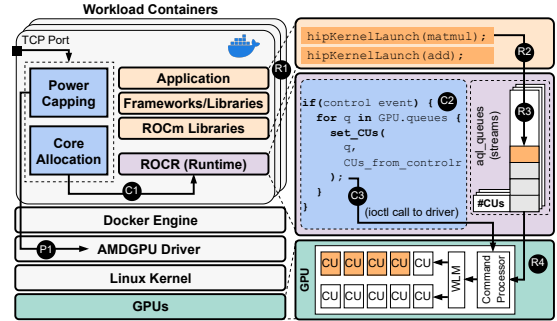


Figure 6: EcoCENTER resource management. Dashed blue boxes show ROCm modifications to provide *power capping* and *core allocations* APIs for the *Controller* to reshape server power.

its power based on the *regulation signal*. At the end of each hour, the power grid credits the data centers with a monetary reward based on the *performance score*, which is taken into account in electricity cost savings on the data center.

We model the exogenous carbon savings (as discussed previously in Section 3) using the aggregate average power of the data center (Data Center P') and the aggregate data center regulation provision (Data Center R).

Maximizing regulation provision: In order to maximize regulation provision, EcoCENTER must have sufficient workload flexibility to modulate without impacting workload QoS. Workloads are either latency-critical (LC) or best-effort (BE). LC workloads tend to offer less flexibility in modulating power due to strict QoS requirements. Therefore, EcoCENTER co-locates LC and BE workloads to enable multi-GPU servers more dynamic power range that can be modulated, which enables greater amount of regulation provision. Frequency regulation signals can request servers to increase power consumption more than the server’s LC workload is currently consuming, thus co-locating LC and BE workloads enable GPU-based servers to modulate power in both directions.

4.2 EcoCenter Workload and Power Monitor

The EcoCENTER *Workload monitor*, a light-weight process within the workload’s docker container, monitors the QoS of LC workloads and passes the performance metrics to the *Controller* to make power reshaping decisions. We used a multi-GPU inference server which load schedules the least amount of GPUs necessary for the current load [61]. Thus, the workload monitor obtains the request inference times, resource requirements, and sends this to the *controller*.

The *Power monitor*, a dockerized service as shown in Figure 5, uses GPU system management (SMI) API along with Turbostat tool, a CPU power measuring tool, to sample the power of the GPU and CPU, respectively. The power samples are published to its corresponding *Controller* every second. The power samples are then used by the *Controller* for power reshaping decisions.

4.3 EcoCenter Resource Manager

The *Resource Manager* executes resource allocation decisions made by the *Controller*. The *Resource Manager* is a light-weight process within the workload’s docker container and controls each GPU

individually by sending different management commands to each. The *Resource Manager* exposes two APIs to the *Controller* for *Power capping API* and *Core allocation API*.

The *Power capping API*, shown in Figure 6, provides an interface to GPU system management interface (SMI)—nvidia-smi (for NVIDIA GPUs) and rocm-smi (for AMD GPUs)—to communicate with the GPU driver P_1 and cap the power consumption of the GPUs with frequency scaling.

The *Core allocation API* component is integrated into the framework to dynamically adjust GPU core allocations to each application. Figure 6 illustrates the integration of the *Core Allocation API* into the ROCm runtime stack for GPU-accelerated workloads. Upon an application’s R_1 GPU kernel launch R_2 , the kernel traverses the GPU runtime stack to be queued R_3 into its designated stream residing in the ROCm runtime for execution on the GPU hardware R_4 . Each queue contains a bitmask (CU Mask³) dictating its kernel allocation across GPU cores. This bitmask is set to all GPU cores by default (e.g. 60 CUs for AMD MI50).

When the *Controller* issues a core allocation command to the *Core Allocation API*, a bitmask is generated by *Resource Manager* and sent into ROCm runtime. To avoid costly Linux sysfs interfaces, we implement a shared memory interface between the *Resource Manager* and ROCm runtime C_1 . We modified the ROCm runtime to intercept kernel execution and manipulate their core allocation bitmask C_2 . The bitmask is applied to all queued kernels through an IOCTL syscall C_3 .

4.4 Power Modulation Knobs for Individual GPU

To reshape server power, ECOCENTER implements a power modulation policy to accurately follow the *regulation signal*. To increase regulation provision, ECOCENTER coordinates *Power capping* and *GPU core allocation* across all GPUs in a multi-GPU server. We first characterize a single GPU’s power modulation knobs and investigate their impact on power modulation precision, workload throughput, and power efficiency.

4.4.1 POWER AND PERFORMANCE MODEL. ECOCENTER constructs a power model for each BE workload, which we use to guide power modulation. Since we do not modulate the LC workload, we do not construct the LC power model and rely on real-time power monitoring. The *Controller* adjusts power levels by utilizing the BE’s power model to issue resource management commands to supplement the LC’s real-time power usage, in line with the regulation signal.

We construct the BE workload’s power model online opportunistically when there are GPU idleness. For a single idle GPU, we run the BE workload with varying power caps and CU masks, and extrapolate a multi-GPU power model. To build the power model, the Controller profiles power consumption data by varying the *Power Cap* and *GPU cores* while recording performance metrics for the workload. Figure 7(a) illustrates the power model for GPT2 training (BE) workload on a single GPU under various GPU cores and power capping constraints. Additionally, the Controller collects the

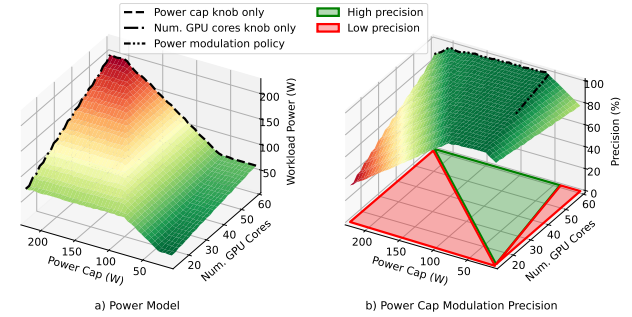


Figure 7: (a) GPT2 model training power model (b) GPT2 model training power cap and number of GPU cores knobs precision (absolute difference of target power and consumed power).

workload’s performance and throughput statistics under different resource constraints.

4.4.2 Choosing the Power Modulation Policy. In Figure 7(a), the dashed line shows the power modulation trend using only power capping. We observe that this knob is suitable for accurately modulating GPU power between ~ 60 – 190 W, but not below ~ 60 . Decreasing the power cap below this point does not significantly decrease GPU power. Note that these power values are for the AMD MI50 and would vary with other GPUs, however, similar power trends exist.

The dash-dotted line in Figure 7(a), shows the power trend of adjusting number of GPU cores with constant maximum power cap. We observe that this knob can modulate down to ~ 60 W, but with low accuracy. From a performance view this knob impacts the performance of the workload more drastically, compared to *power capping*, since workloads are more sensitive to resource count than operating frequency. We observe core allocation knob degrades the workload throughput by up to $\sim 80\%$ while power capping degrades up to $\sim 40\%$.

How to provide high quality power modulation? We evaluate the precision (absolute difference of target power and actual consumed power) of using power capping to modulate the server power. Figure 7(b) illustrates the quality of the power capping knob. **To overcome the inaccuracies of GPU power knobs [9], we use GPU core scaling to fine-tune the modulated power of power capping.** The red regions show power modulation precision $< 90\%$ (low precision) and the green region with $> 90\%$ (high precision). The power modulation policy aims to provide high quality power modulation, with $\geq 90\%$ precision, within the green region.

How to navigate through high precision area to modulate power? The difference in impact of *core allocation* and *power capping* knobs on workload performance/throughput is leveraged in power modulation policy implemented in EcoCENTER. Since the impact of power capping knob on the workload’s performance is almost half of that of number of GPU cores, EcoCENTER controller first modulates with power capping then core allocation to fine-tune the power.

Limitations of Single GPU Power Modulation Knobs. Following the above policies for individual GPUs, *each GPU still contain ~ 60 W of untapped power range that can further contribute*

³While we target AMD’s CU Masking for resource scaling, similar features exist for Nvidia GPUs with Green Context [62] and libsmctrl [63].

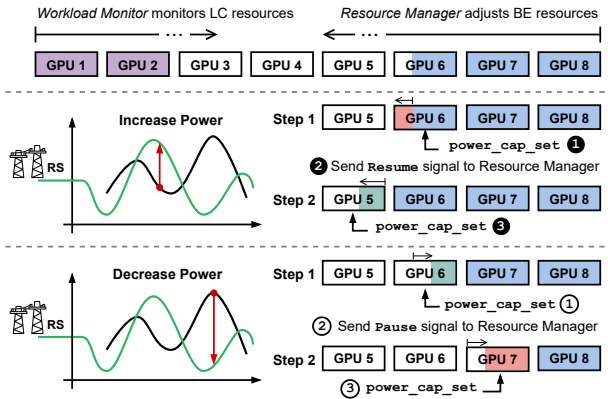


Figure 8: ECOCENTER power reshaping policy with 8 GPUs. *Workload Monitor* monitors the LC resources, while *Resource Manager* (directly by *Controller*) reshapes the BE workload.

to regulation provision. Unlike CPUs, which includes a plethora of low-power state knobs (DVFS, C-states, fine-grain power gating, preemption, etc.) to optimize non-peak utilization, GPU's power knobs are limited to power capping and CU scaling, but lacks fine-grain power gating, which provides more dynamic power range at low power range. Thus, we require further mechanisms to increase regulation provision.

4.5 Coordinating Multiple GPUs to Maximize Frequency Regulation Provision

To maximize regulation provision with GPU's limited power modulation knob, the ECOCENTER *Controller* coordinates both LC and BE workloads, along with the GPU's power cap and core allocation knob. Although individually these knobs can achieve 2 second responsiveness, the challenge is to coordinate these across multiple GPUs to meet the 2-second responsiveness while maximizing regulation provision.

The *Controller* reads the real-time power broadcasted by *Power Monitor* and based on the regulation signal, it calculates the required target server power. Our assumption is that the LC workloads fluctuate unimpeded over time with varying number of GPUs to support the required load. Rather than co-locating other LC workloads to improve under-utilization, EcoCENTER schedules BE workloads to fill in the under-utilization and modulates it for regulation service. Thus, to maximize the amount of regulation provision, EcoCENTER carefully coordinate the GPUs by LC and BE groups. Figure 8 illustrates an overview of power reshaping policy.

LC and BE GPU allocation: On the LC workload side, the *Workload Monitor* is configured to allocate GPUs to the LC workload unobstructed (purple) from lower GPU index (1) to higher index GPUs (8) based on the current load of the server. For example, as the LC workloads fluctuate, it grows from GPU 1 to higher number GPUs. To avoid BE and LC interference, the BE workload's GPU resources are allocated starting from GPU with the highest index toward GPUs with lower index. For example, in Figure 8, BE workload's GPUs (shown in blue) are allocated from GPU 8 towards lower indexed GPUs for modulation. The *Workload monitor* track

how many GPUs are required for the LC workload and dynamically free available GPUs to BE workloads.

Decreasing server power: The controller decreases server power by issuing a *power_cap_set* command ① to *Resource Manager* with a target power value lower than the current GPU power, until that GPU's minimum controllable power level. The issued target power value is calculated based on the profiled power model for the deployed BE workload. The power can further be decreased by issuing a pause command ② to pause the GPU's workload, which can effectively remove the ~60W of untapped power range as previously described. Once paused, we can continue decreasing power by again calling *power_cap_set* command ③ to the next GPU to further decrease server power.

Increasing server power: Conversely, the red sections in Figure 8 show how server power is increased by adjusting GPU resources of the BE workload. The *Controller* increases the server power by issuing a *power_cap_set* command ① to *Resource Manager* with a target power value higher than the current GPU power. The power cap increment is continued until it reaches that GPU's maximum power.

To further increase the power, the *Controller* issues a resume command ② to *Resource Manager* to resume the BE workload processes running on the next GPU followed by a *power_cap_set* with the minimum power cap value for the GPU ③. This results in an immediate ~60W jump in server power, so we adjust the other GPU's power accordingly to provide the necessary precision to meet server target power.

Resuming and Pausing BE Workloads: By coordinating multiple GPUs and resuming/pausing GPUs, we can tap into extra GPU power range (~60W per GPU) that can be leveraged for regulation provision. To pause/resume individual GPUs, we run multiple single-GPU BE workloads, which is reflective of real clouds where most workloads are single GPU [64]. When a training job on the GPU is paused, we stop issuing of new kernels to the GPU, which allows the GPU to go into an active idle state to achieve a lower near-zero power consumption. This is achieved through the ROCm runtime where we simply pause the issuing of kernels in the *aql_queues* (Figure 6 R4). When paused, memory state is retained in the GPU memory since the GPU is not completely powered off but in an active idle state. This way, the job can readily resume by reissuing kernels to the GPU.

4.6 EcoCenter Optimizer

As mentioned in Section 2.3, we utilize the CAISO real-time market. CAISO allows for asymmetric bidding and provides two different prices for regulation rewards: Up Regulation reward (rew_{up}) for decreasing power consumption, and Down Regulation reward (rew_{down}) for increasing power consumption. We optimize the power consumption cost of a server participating in frequency regulation ($P_{f.r.}$) and the provided regulation provision by extending the optimization formulation proposed by [6] to provide asymmetric regulation provision (R_{up} and R_{down}). Equation (2) shows the formulation of the server with workload that consumes P_{avg} power and the power variation (due to fluctuations in load) P_{var} .

$$\begin{aligned}
\text{Maximize : } & \text{Saving} = \text{Cost}_{P_{avg}} - \text{Cost}_{f.r.} \\
\text{such that : } & \text{Cost}_{P_{avg}} = \underline{P_{avg}} \times \underline{\text{cost}} \\
& \text{Cost}_{f.r.} = \underline{P_{f.r.}} \times \underline{\text{cost}} - \text{Reward} \times \underline{\text{perf. score}} \\
& \text{Reward} = \underline{R_{up}} \times \underline{\text{rew}_{up}} + \underline{R_{down}} \times \underline{\text{rew}_{down}} \\
& \text{Cost}_{f.r.} \leq \text{Cost}_{P_{avg}} \times \underline{\text{threshold}} \\
& 0 \leq \underline{R_{down}} \leq \underline{P_{max}} - \underline{P_{f.r.}} \quad (2) \\
& 0 \leq \underline{R_{up}} \leq \underline{P_{f.r.}} - (\underline{P_{avg}} + \frac{\underline{P_{var}}}{2}) \\
& \underline{P_{avg}} + \frac{\underline{P_{var}}}{2} < \underline{P_{f.r.}} < \underline{P_{max}} \\
\text{if symmetric provision : } & \underline{R_{up}} = \underline{R_{down}}
\end{aligned}$$

In the optimization formulation of Eq. (2), the **bold** parameters are outputs and underlined parameters are inputs. The primary aim is to maximize savings by minimizing the difference between the average power cost ($\text{Cost}_{P_{avg}}$) and the frequency regulation cost ($\text{Cost}_{f.r.}$). The average power cost ($\text{Cost}_{P_{avg}}$) is determined by the product of the average power consumption (P_{avg}) and the unit cost of power (cost). On the other hand, the frequency regulation cost is influenced by the power allocated for frequency regulation ($P_{f.r.}$), the cost per unit power (cost), and a performance score factor (perf. score). This cost is offset by rewards (Reward) from regulation activities, which include the up or down regulation provision (R_{up} or R_{down}). These rewards are multiplied by their respective reward values (rew_{up} , rew_{down}).

Constraints ensure that the regulation cost doesn't exceed a specified *threshold*, and that regulation provisions (R_{up} and R_{down}) and power allocations remain within feasible bounds. The threshold parameter provides flexibility for data center operators to specify a threshold of savings to decide whether to participate in frequency regulation or withdraw from the service based on the state of the data center. The last 3 lines add constraints to ensure that the regulation provision upper range does not exceed the server's max power, the regulation provision lower range does not overflow into the LC workload's power range, and whether the ISO provides symmetric or asymmetric frequency regulation. This formulation also can be utilized if symmetric provision is required, for markets such as PJM, where the regulation up (R_{up}) and down (R_{down}) capacities are enforced to be equal.

We utilize the Z3 SAT solver [65] to solve this optimization problem hourly to obtain the amount of regulation the data center will provide in the next hour. We observe that this optimization formulation can be solved by Z3 in the order of tens of seconds.

5 Evaluation

5.1 Evaluation Methodology

5.1.1 Experimental Setup and Benchmarks. We utilize a server with 8 AMD MI50 GPUs, a 16-core AMD EPYC 7302 processor, and 512GB of DRAM. The power consumption was monitored using rocm-smi [66] and TurboStat.

For our latency-sensitive workload, we run the Resnet152 model on a multi-GPU machine learning inference server [67] as a representative workload. We define the 95th percentile tail latency of the inference workload running independently by identifying the "knee" of the utilization-tail latency curve, similar to established methodologies [68, 69]. For our best-effort workload, we use

GPT-2 [70] training. We measured the BE's throughput as training iterations per second (iter/sec). **Since ECOCENTER does not modulate any latency-sensitive workloads, the goal here is to demonstrate that latency-sensitive workloads are untouched and should generalize to other latency-sensitive workloads. As long as a BE workload can be modulated (our modulation knobs are application-agnostic and hardware-based), we can also generalize BE workloads.** To test generalizability, we ran experiments with Albert inference (LC) and hipBLAS (BE) and observe similar trends, but omit detailed results for brevity.

In our evaluation, the *Baseline* scenario co-locates LC and BE workloads without regulation service, unless otherwise indicated. While the LC workload fluctuates, the BE workload is able to grow and fill up the under-utilized GPU resources in the server. The ECOCENTER scenario utilize the BE workloads for regulation service by modulating GPU power and multi-GPU coordination as discussed previously. For certain evaluations, we also evaluate a *CPU-only regulation service* scenario similar to PowerMorph [6], which modulates a BE workload through CPU core isolation and DVFS. We also evaluate a *PowerMorph-GPU* policy that naively applies PowerMorph's policy onto GPUs (which modulates a BE workload through CU isolation and does not support multi-GPU coordination), and a *UPS-only regulation service* where regulation service is provided by the UPS battery backups.

Table 1: Workload utilization traces from the Facebook SWIM trace [71] with combinations of load and variation.

Trace (Mean-Var)	Mean(%)	Var.	Min (%)	Max (%)
low-low	28.66	12.48	23	36
low-med	28.86	16.78	23	40
low-high	29.33	22.62	24	42
med-low	42.13	6.51	37	46
med-med	50.13	46.64	35	63
med-high	51.66	177.55	36	73
high-low	73.33	103.42	55	94
high-med	72.33	116.22	55	92
high-high	70.73	144.99	52	91

5.1.2 Workload Utilization Traces. We evaluate under realistic varying workload utilization traces of Facebook SWIM project [71] listed in Table 1. The traces are selected from 1-hour windows of the SWIM project trace to demonstrated a combination of *load levels* where the mean load is low (30%), medium (50%), high (70%), and the *load variation* is low, medium and high variance. The LC workloads follow this utilization trace, while the BE workload either fills all under-utilization (baseline) or fill in the utilization gap to track regulation signal.

5.1.3 Regulation Signal Selection. We select three regulation signals from PJM, similar to prior work [6]. Figure 9 shows the regulation signals. Since we are participating in the hour-ahead regulation market, we picked one-hour slices. We chose Extreme (E) with a regulation signal that stays in the highest and the lowest power points for extended periods of time, High Transition (HT) which features frequent min-to-max power change requests, and Noisy (N) to evaluate how accurately ECOCENTER can track small frequent changes.

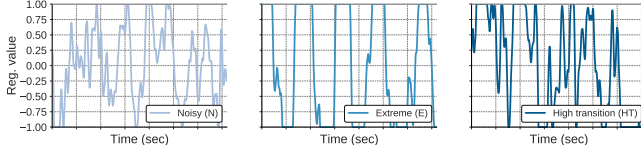


Figure 9: Regulation signals used in evaluation with varying volatility (Noisy, Extreme, High Transition)[6].

Table 2: ECOCENTER regulation service performance score.

Load Trace	Regulation Signal			Avg
	Extreme (E)	Noisy (N)	High Trans. (HT)	
low-low	96.72	96.10	96.99	96.60
low-med	96.94	96.50	96.95	96.80
low-high	96.60	96.06	96.84	96.5
med-low	95.79	95.56	95.50	95.62
med-med	93.02	93.62	93.38	93.34
med-high	93.84	93.64	94.69	94.05
high-low	85.36	85.15	86.36	85.62
high-med	84.10	81.07	85.82	83.66
high-high	84.94	82.34	84.76	84.01

5.1.4 *Electricity Cost and Regulation Reward Selection.* We analyzed the electricity rewards and regulation reward data from CAISO for the year 2022 and performed clustering to identify eight weeks that provide the best coverage of typical electricity market electricity cost and regulation reward across that year. We use this to evaluate Total Cost of Ownership (TCO) and electricity cost.

5.1.5 *Carbon modeling.* We assume each GPU’s carbon emission footprint is 30 kg CO₂eq, with CPU, DRAM and disk having 18, 7, and 20 kg CO₂eq, respectively [40]. To scale this to the data center-level, we scale the per-server carbon footprint by the number of servers that can fit within the data center’s power capacity. We further amortize the embodied carbon over 5 years [18]. We assume a 100MW capacity data center in our evaluation. We also assume there exist sufficient UPS battery for 1 hour of backup with 100MWh of capacity with carbon footprint of 74 tons CO₂eq per MWh [13].

For operational carbon (without regulation service), we utilize the CarbonExplorer [13] framework. We will evaluate both the *simplified exogenous carbon model* and the *detailed grid-based exogenous carbon model*. For the simplified exogenous carbon model’s MCE_{resv}, we evaluate two extreme cases where the regulation reserve is either a gas power plant or battery. Detailed exogenous carbon modeling was discussed in Section 3.1.

5.2 Evaluation Results

Performance Score: Table 2 presents the average performance scores [34] for providing regulation service across different scenarios. The lowest performance score is observed with the Noisy regulation signal, which has the most intermediate (non-max or min) regulation signal values, which presents the most challenge for precise power modulation. Performance score tends to decrease with higher utilization traces, all observing less than 80%. At high loads, there are less dynamic power range available for frequency regulation, thus, making regulation signal tracking more challenging. ECOCENTER consistently achieves scores above 80%, with an overall average of 91.20%. This demonstrates that ECOCENTER is able to accurately modulate power at 2-second granularity and provide high-quality regulation service.

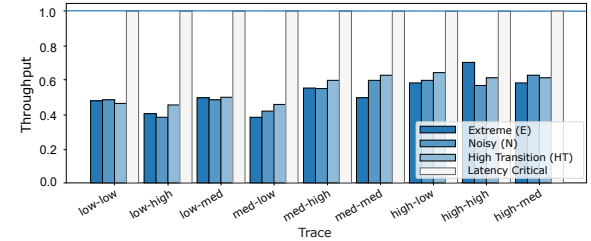


Figure 10: Normalized throughput for ECOCENTER w.r.t the baseline with Facebook SWIM [71] traces. BE workloads are in blue and are sensitive to regulation traces.

Workload Throughput: Figure 10 illustrates the normalized throughput (y-axis) of both LC and BE workloads under different workload traces (x-axis) and regulation signals (series). Since LC workload’s resources are preserved, the throughput is unaffected. For BE workloads, the workload is used to modulate the power to match the regulation signal. Since the workload is modulated, the BE workload naturally experiences reduced throughput compared to the baseline where the BE workload runs unmodulated. With higher workload load, the amount of regulation provision decreases, leading to higher throughput for BE workloads. Since we’re modulating the workload around a regulation signal, one would expect the BE throughput to hover around 50%. In general, we observe more throughput impact for Extreme and Noisy regulation signals, since the signal tends to be negative more often, requiring more throttling of BE workloads. In the remainder of the evaluation section, we will conservatively evaluate on the Noisy regulation signal since it is the most challenging, unless otherwise stated.

Workload Latency: Since the LC workload is not actively modulated and runs on a distinct set of GPUs compared to the BE workload, we do not see any noticeable differences in workload latency when running with and without regulation service. For brevity, we omit a latency figure.

Regulation Provision: Figure 12 shows the amount of regulation provision provided by ECOCENTER, PowerMorph on CPUs, and PowerMorph on GPUs. All results are normalized to PowerMorph on GPUs. Since GPUs consume significantly more power than CPUs in data centers, ***we observe that both GPU-based frequency regulation framework achieves >3x more regulation provision than CPUs alone***, providing significant power flexibility. As utilization increases, the amount of regulation provision shrinks. Going from 10% to 50%, and 50% to 80% utilization, the amount of regulation provision we observe (not illustrated in figure) decreased by 22% and 56%, respectively for PowerMorph-CPU, and 16% and 35%, respectively for PowerMorph-GPU, and 13% and 26% respectively for ECOCENTER. ECOCENTER is able to coordinate across multiple GPUs to squeeze out regulation provision opportunities, allowing sustained regulation provision at higher loads compared to PowerMorph applied to GPU. ECOCENTER provides ~30% to 50% more regulation provision compared to PowerMorph-GPU and 4x (up to 7x at high util.) compared to PowerMorph-CPU.

Exogenous Carbon Saving: Figure 11 shows the annualized carbon emission components for a data center with a 100MW capacity under various operational loads (10%, 50%, and 80%). ECOCENTER is compared to a *baseline scenario where only the LC workload*

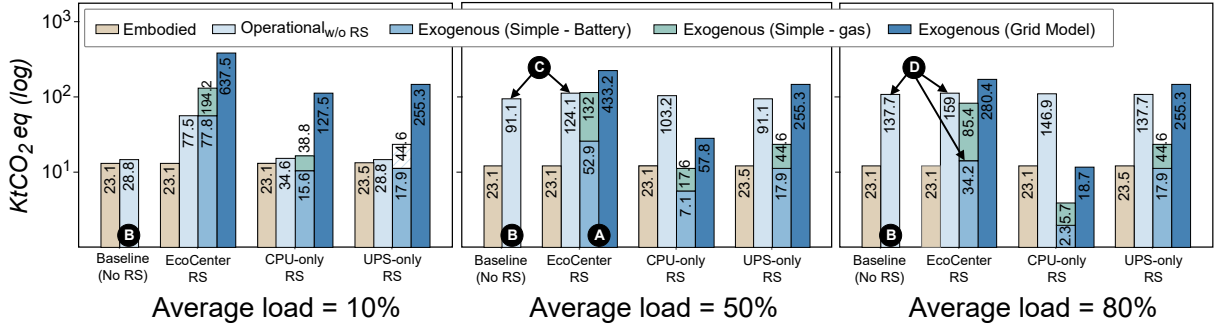


Figure 11: Comparison of Exogenous carbon savings with data center carbon emissions at different operational loads.

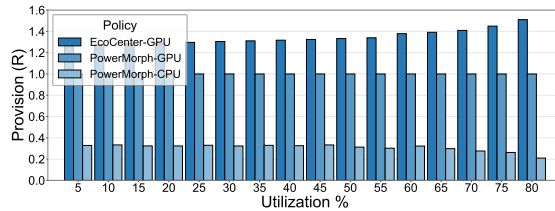


Figure 12: Amount of data center regulation provision normalized to PowerMorph-GPU.

is running so we can tease out the operational carbon due to the energy increase used for power modulation of the BE workload⁴. We also compare against a CPU-only [6] and a UPS-only regulation service (RS), where we assume 20% of the UPS capacity is used for regulation service to keep battery capacity for backup. Embodied carbon is amortized over 5 years and remains consistent across all scenarios except for UPS-only RS due to the battery lifetime impact. Prior works observe that batteries deployed in regulation service experience a 28% shorter lifespan [72].

Similarly, to tease out the impact on grid-side regulation reserve emission benefits, we report operational carbon without regulation service, C_{op} , and the exogenous carbon term, $C_{\text{exogenous}}$, separately instead of the combined $C_{\text{op}w/\text{RS}}$ (Eq. 1). Operational carbon is estimated from the average datacenter power obtained from representative 10%, 50%, and 80% load traces for LC workloads. Embodied carbon is independent of load. The load impacts the amount of regulation provision (Figure 12) to modulate the BE workload based on regulation signals and thus, impacts Exogenous carbon savings.

As we discussed previously in Section 3.1, when data centers provide regulation service, we see an out-sized impact to grid-side carbon emissions savings. We observe this where the grid model-based exogenous carbon benefits are often significantly higher (3x) than a simple exogenous carbon model (e.g. ① 433.2 kt CO₂eq vs. 132 kt CO₂eq for EcoCenter RS at 50% load.), highlighting the need to consider high-fidelity modeling of grid-side dynamics.

Operational carbon increases with higher loads (e.g. ① 28.8 kt CO₂eq vs 91.1 kt CO₂eq vs 137.7 kt CO₂eq for Baseline as load increases). With EcoCenter and CPU-only RS, modulating co-located

⁴If we assume the baseline scenario already runs co-located BE workloads to improve GPU utilization, then regulation service would observe reduction to both operational carbon and grid-side exogenous carbon, with the trade-off being throughput (Figure 10). We evaluate a Baseline of LC-only, which leads to a conservative estimate of EcoCenter's carbon emissions benefits.

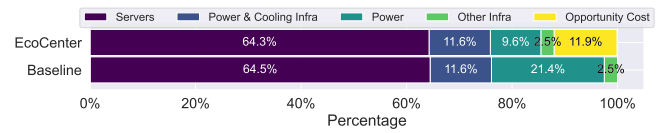


Figure 13: TCO breakdown showing CapEx (Servers, Infra), OpEx (Power), and Opportunity cost.

BE workloads also leads to operational carbon increase of running BE workloads compared to a baseline with LC-only workloads. For example, with 50% load, the operational carbon ② increases from 91.1 to 124.1 kt CO₂eq due to BE workloads for modulation. This increase is *completely outweighed by the grid-side exogenous carbon savings of ① 52.9-433.2 kt CO₂eq*. **In all scenarios, grid-side exogenous carbon savings completely outweighs the operational carbon increase for regulation service**, matching or improving on the emissions of an LC-only baseline.

Exogenous carbon savings decline as the load increases, reflecting reduced flexibility in providing regulation provisions (Figure 12). Even in the worse-case with 80% load, EcoCenter's grid-side exogenous carbon saving of 34.2 kt CO₂eq ③ still outweighs the operational carbon increase of 21.3 kt CO₂eq, resulting in net carbon emission improvement of 12 kt CO₂eq. In general, **the exogenous carbon benefits of CPU-only RS is very limited, and degrades quickly with load increase**. While UPS-only RS provide better exogenous carbon benefits than CPU-only RS, but still lags EcoCenter.

In certain scenarios (at 10% load), the amount of grid-side exogenous carbon benefits *completely outweigh* the datacenter's carbon footprint, where the amount of grid-side exogenous carbon saved exceeds the data center's operational and embodied carbon footprint. At low load, data centers can provide a significant amount of regulation provision.

Total Cost of Ownership: To evaluate TCO, we follow the methodology of [73, 74] and model a 100MW data center with facility construction cost of \$8 per W [74] amortized over 15 years and PUE of 1.09 [75]. We model server cost as state-of-the-art 8-GPU servers costing \$235K each requiring 7KW per server [76]. We evaluate a range of electricity cost from \$0.05 to \$0.30 per kWh. For reward pricing, through historical CAISO electricity and reward pricing, we find the average reward pricing for a certain electricity cost level, which we observe to average around \$7/MW [77]. Since



Figure 14: Normalized TCO w.r.t. baseline data center shows a fundamental trade-off of opportunity cost.

regulation service modulates BE workloads, we also capture the cost of this lost throughput as *opportunity cost*. We model opportunity cost from the amount of GPU hours lost and the hourly cost of a cloud GPU instance.

Figure 13 shows the cost breakdown of data centers with and without EcoCENTER. In general, capital expenses (servers, power and cooling infrastructure, other infrastructure) remains the same. Operational expenses differ due to data centers receiving monetary rewards for participating in regulation service, hence the lower power cost component. However, this comes at the cost of opportunity cost where EcoCENTER trade-off throughput of BE workloads in order to modulate power. This fundamental trade-off between opportunity cost and power cost (OpEx) drives the overall TCO picture.

Figure 14 shows the TCO of EcoCENTER normalized to baseline. As electricity cost increases, it becomes a bigger component of TCO and thus can benefit from more rewards pricing, resulting in lower TCO. As the cost per GPU hour increases, we observe that opportunity cost begins to dominate and eventually outweighs the OpEx benefits and observe negative TCO impact. Therefore, to limit opportunity cost, frequency regulation is best done with lower cost per GPU hour resources while higher cost per GPU hour resources can still be dedicated towards latency-sensitive workloads, such as inference, without impacting its performance.

6 Related Work

Frequency regulation in data centers: Previous data center frequency regulation service works target techniques such as DVFS, stored energy devices, and coordinating local power generators, primarily target batch workloads and operate on 15-minute intervals, which are insufficient for the 2-second adjustments required for frequency regulation [6, 8, 36–38, 78, 79]. PowerMorph [6] addresses this with millisecond-level QoS. However, it targets CPU only which limits the amount of regulation provision in modern data centers. Additionally, using UPS systems for regulation services is costly and reduces their lifespan, as they are primarily designed for backup power [80].

Other demand response in data centers: Significant prior works have explored data center demand response services at hourly-granularity to improve the reliability of power grids under stress, such as load shedding during power emergencies or load shifting. There are several strategies, such as temporal and spatial load shifting/job migration [7, 14–17, 28], voluntary load reduction and power capping [81], through techniques like Dynamic Voltage

and Frequency Scaling (DVFS) [82, 83], thread packing [83, 84], and co-scheduling [85–87]. These traditional data center demand response mechanisms cannot be directly applied to provide frequency regulation services as solutions require hour-scale responsiveness and cannot be responsive at second-scale.

Carbon-aware data centers: Many prior studies, have explored carbon-aware policies, such as temporal and spatial (geographical) workload shifting, carbon-aware scheduling, net-zero data centers, etc. [15–17, 24–31]. More recently, Carbon Explorer [13] explores the trade-off between reducing operational carbon and increasing embodied carbon from infrastructure manufacturing. Carbon Responder [14], proposed a framework that develops performance-aware power allocation policies to reduce carbon emissions during periods of high grid carbon intensity. While these prior works are aware of the power grid’s carbon intensity, these prior works do not actively participate to improve grid reliability or account for carbon emissions of regulation reserves.

7 Conclusion

This work demonstrates how data centers can decrease reliance on fossil fuel-based regulation reserves. We introduce Exogenous Carbon to capture the grid-side carbon savings due to data center regulation service. We introduced EcoCenter, a framework to maximize regulation provision and provide accurate regulation service. EcoCenter can achieve high-quality regulation, lower TCO, and in certain scenarios, achieve grid-side exogenous carbon savings that completely outweighs the operational carbon of the data center.

References

- [1] J. Aljbour, T. Wilson, and P. Patel, "Powering intelligence: Analyzing artificial intelligence and data center energy consumption," *EPRI White Paper*, 2024.
- [2] M. Stanley, 2023. [Online]. Available: <https://www.datacenterdynamics.com/en/news/morgan-stanley-data-center-industry-will-emit-25bn-tons-of-co2-by-2030/>
- [3] Google, "Environmental report," 2023. [Online]. Available: <https://www.gstatic.com/gumdrop/sustainability/google-2023-environmental-report.pdf>
- [4] Microsoft, "Powering sustainable transformation," 2025. [Online]. Available: <https://datacenters.microsoft.com/globe/powering-sustainable-transformation/>
- [5] U. E. I. A. (EIA), "Electricity data browser," <https://www.eia.gov/electricity/data-browser/>, 2023.
- [6] A. Jahanshahi, N. Yu, and D. Wong, "Powermorph: Qos-aware server power reshaping for data center regulation service," *ACM Transactions on Architecture and Code Optimization (TACO)*, vol. 19, no. 3, pp. 1–27, 2022.
- [7] Google, "Supporting power grids with demand response at google data centers," 2023. [Online]. Available: <https://cloud.google.com/blog/products/infrastructure/using-demand-response-to-reduce-data-center-power-consumption>
- [8] H. Chen, Y. Zhang, M. C. Caramanis, and A. K. Coskun, "EnergyQARE: QoS-Aware Data Center Participation in Smart Grid Regulation Service Reserve Provision," *ACM Trans. Model. Perform. Eval. Comput. Syst.*, vol. 4, no. 1, pp. 2:1–2:31, Jan. 2019. [Online]. Available: <http://doi.acm.org/10.1145/3243172>
- [9] P. Patel, Z. Gong, S. Rizvi, E. Choukse, P. Misra, T. Anderson, and A. Sriramam, "Towards improved power management in cloud gpus," *IEEE Computer Architecture Letters*, vol. 22, no. 2, pp. 141–144, 2023.
- [10] G. Cook, E. Jardim, and C. Craighill, "Clicking clean virginia the dirty energy powering data center alley," *Greenpeace Available from: https://www.greenpeace.org/usa/reports/click-clean-virginia/[Accessed 21 Mar 2020]*, 2019.
- [11] "Ai is poised to drive 160% increase in data center power demand," 2024. [Online]. Available: <https://www.goldmansachs.com/insights/articles/AI-poised-to-drive-160-increase-in-power-demand>
- [12] H. Touvron, L. Martin, K. Stone, P. Albert, A. Almahaire, Y. Babaei, N. Bashlykov, S. Batra, P. Bhargava, S. Bhowse *et al.*, "Llama 2: Open foundation and fine-tuned chat models," *arXiv preprint arXiv:2307.09288*, 2023.
- [13] B. Acun, B. Lee, F. Kazhamiaka, K. Maeng, U. Gupta, M. Chakkavarthy, D. Brooks, and C.-J. Wu, "Carbon explorer: A holistic framework for designing carbon aware datacenters," in *Proceedings of the 28th ACM International Conference on Architectural Support for Programming Languages and Operating Systems, Volume 2*, 2023, pp. 118–132.
- [14] J. Xing, B. Acun, A. Sundararajan, D. Brooks, M. Chakkavarthy, N. Avila, C.-J. Wu, and B. C. Lee, "Carbon responder: Coordinating demand response for the datacenter fleet," 2023. [Online]. Available: <https://arxiv.org/abs/2311.08589>
- [15] H. Dou, Y. Qi, W. Wei, and H. Song, "Carbon-aware electricity cost minimization for sustainable data centers," *IEEE Transactions on Sustainable Computing*, vol. 2, no. 2, pp. 211–223, 2017.
- [16] J. Luo, L. Rao, and X. Liu, "Temporal load balancing with service delay guarantees for data center energy cost optimization," *IEEE Transactions on Parallel and Distributed Systems*, vol. 25, no. 3, pp. 775–784, 2013.
- [17] T. Sukprasert, A. Souza, N. Bashir, D. Irwin, and P. Shenoy, "On the limitations of carbon-aware temporal and spatial workload shifting in the cloud," in *Proceedings of the Nineteenth European Conference on Computer Systems*, ser. EuroSys '24. New York, NY, USA: Association for Computing Machinery, 2024, p. 924–941. [Online]. Available: <https://doi.org/10.1145/3627703.3650079>
- [18] B. Li, S. Samsi, V. Gadepally, and D. Tiwari, "Clover: Toward sustainable ai with carbon-aware machine learning inference service," in *Proceedings of the International Conference for High Performance Computing, Networking, Storage and Analysis*, 2023, pp. 1–15.
- [19] GreenTechMedia, "In california, solar and wind boost the price of frequency regulation," 2022. [Online]. Available: <http://www.greentechmedia.com/articles/read/in-california-solar-and-wind-boosts-the-price-for-frequency-regulation>
- [20] P. Alstone, J. Potter, M. A. Piette, P. Schwartz, M. A. Berger, L. N. Dunn, S. J. Smith, M. D. Sohn, A. Aghajanzadeh, S. Stensson *et al.*, "2025 california demand response potential study-charting california's demand response future. final report on phase 2 results," Lawrence Berkeley National Lab.(LBNL), Berkeley, CA (United States), Tech. Rep., 2017.
- [21] Y. Zhang, I. C. Paschalidis, and A. K. Coskun, "Data center participation in demand response programs with quality-of-service guarantees," in *Proceedings of the Tenth ACM International Conference on Future Energy Systems*, 2019, pp. 285–302.
- [22] Y. Zhang, D. C. Wilson, I. C. Paschalidis, and A. K. Coskun, "Hpc data center participation in demand response: An adaptive policy with qos assurance," *IEEE Transactions on Sustainable Computing*, vol. 7, no. 1, pp. 157–171, 2022.
- [23] A. Wierman, Z. Liu, I. Liu, and H. Mohsenian-Rad, "Opportunities and challenges for data center demand response," in *International Green Computing Conference*, 2014, pp. 1–10.
- [24] C. Li, A. Qouneh, and T. Li, "Iswitch: Coordinating and optimizing renewable energy powered server clusters," in *Proceedings of the 39th Annual International Symposium on Computer Architecture*, ser. ISCA '12. USA: IEEE Computer Society, 2012, p. 512–523.
- [25] I. Goiri, K. Le, M. E. Haque, R. Beauchea, T. D. Nguyen, J. Guitart, J. Torres, and R. Bianchini, "Greenslot: scheduling energy consumption in green datacenters," in *International Conference for High Performance Computing, Networking, Storage and Analysis*, 2011.
- [26] C. Li, W. Zhang, C. Cho, and T. Li, "Solarcore: Solar energy driven multi-core architecture power management," in *2011 IEEE 17th International Symposium on High Performance Computer Architecture*, Feb 2011, pp. 205–216.
- [27] C. Li, X. Li, R. Wang, T. Li, N. Goswami, and D. Qian, "Chameleon: Adapting throughput server to time-varying green power budget using online learning," in *International Symposium on Low Power Electronics and Design (ISLPED)*, Sep. 2013, pp. 100–105.
- [28] Z. Liu, M. Lin, A. Wierman, S. H. Low, and L. L. Andrew, "Geographical load balancing with renewables," *SIGMETRICS Perform. Eval. Rev.*, vol. 39, no. 3, p. 62–66, Dec. 2011. [Online]. Available: <https://doi.org/10.1145/2160803.2160862>
- [29] L. Lin and A. A. Chien, "Adapting datacenter capacity for greener datacenters and grid," in *Proceedings of the 14th ACM International Conference on Future Energy Systems*, 2023, pp. 200–213.
- [30] W. A. Hanafy, Q. Liang, N. Bashir, D. Irwin, and P. Shenoy, "Carbonscaler: Leveraging cloud workload elasticity for optimizing carbon-efficiency," *Proc. ACM Meas. Anal. Comput. Syst.*, vol. 7, no. 3, Dec. 2023. [Online]. Available: <https://doi.org/10.1145/3626788>
- [31] N. Bashir, V. Gohil, A. B. Subramanya, M. Shahrad, D. Irwin, E. Olivetti, and C. Delimitrou, "The sunk carbon fallacy: Rethinking carbon footprint metrics for effective carbon-aware scheduling," in *Proceedings of the 2024 ACM Symposium on Cloud Computing*, ser. SoCC '24. New York, NY, USA: Association for Computing Machinery, 2024, p. 542–551. [Online]. Available: <https://doi.org/10.1145/3698038.3698542>
- [32] California ISO, "Greenhouse gas emission tracking methodology," Tech. Rep., 2016.
- [33] —, "Greenhouse gas coordination stakeholder recommendations for policy development," Tech. Rep., 2024.
- [34] PJM, "PJM Manual 12: Balancing Operations," <https://www.pjm.com/-/media/documents/manuals/m12.aspx>, 2022.
- [35] A. Sadeghi-Mobarak and H. Mohsenian-Rad, "Performance accuracy scores in caiso and miso regulation markets: A comparison based on real data and mathematical analysis," *IEEE Transactions on Power Systems*, vol. 33, no. 3, pp. 3196–3198, 2018.
- [36] H. Chen, M. C. Caramanis, and A. K. Coskun, "The data center as a grid load stabilizer," in *19th Asia and South Pacific Design Automation Conference (ASP-DAC)*. Singapore: IEEE, Jan. 2014, pp. 105–112. [Online]. Available: <http://ieeexplore.ieee.org/document/6742874/>
- [37] H. Chen, C. Hankendi, M. C. Caramanis, and A. K. Coskun, "Dynamic Server Power Capping for Enabling Data Center Participation in Power Markets," in *Proceedings of the International Conference on Computer-Aided Design*, ser. ICCAD '13. Piscataway, NJ, USA: IEEE Press, 2013, pp. 122–129.
- [38] H. Chen, M. C. Caramanis, and A. K. Coskun, "Reducing the data center electricity costs through participation in smart grid programs," in *International Green Computing Conference*, Nov. 2014, pp. 1–10.
- [39] P. Patel, E. Choukse, C. Zhang, I. n. Goiri, B. Warrier, N. Mahalingam, and R. Bianchini, "Characterizing power management opportunities for llms in the cloud," in *Proceedings of the 29th ACM International Conference on Architectural Support for Programming Languages and Operating Systems, Volume 3*, ser. ASPLOS '24. New York, NY, USA: Association for Computing Machinery, 2024, p. 207–222. [Online]. Available: <https://doi.org/10.1145/3620666.3651329>
- [40] B. Li, R. Basu Roy, D. Wang, S. Samsi, V. Gadepally, and D. Tiwari, "Toward sustainable hpc: Carbon footprint estimation and environmental implications of hpc systems," in *Proceedings of the International Conference for High Performance Computing, Networking, Storage and Analysis*, 2023, pp. 1–15.
- [41] J. Lindberg, Y. Abdennadher, J. Chen, B. C. Lesieutre, and L. Roald, "A guide to reducing carbon emissions through data center geographical load shifting," in *Proceedings of the Twelfth ACM International Conference on Future Energy Systems*, ser. e-Energy '21, 2021.
- [42] A. Lacoste, A. Luccioni, V. Schmidt, and T. Dandres, "Quantifying the carbon emissions of machine learning," 2019. [Online]. Available: <https://arxiv.org/abs/1910.09700>
- [43] "The leading api for granular electricity data reduce carbon emissions with actionable electricity data," 2024. [Online]. Available: <https://www.electricitymaps.com>
- [44] J. Gorka, N. Rhodes, and L. Roald, "Electricityemissions.jl: A framework for the comparison of carbon intensity signals," 2024. [Online]. Available: <https://arxiv.org/abs/2411.06560>
- [45] T. Sukprasert, A. Souza, N. Bashir, D. Irwin, and P. Shenoy, "On the limitations of carbon-aware temporal and spatial workload shifting in the cloud," in *Proceedings*

of the Nineteenth European Conference on Computer Systems, ser. EuroSys '24, 2024.

[46] S. Seachman, "Process control strategies for reducing the minimum load of fossil-fired plants," 2025. [Online]. Available: <https://www.powermag.com/process-control-strategies-for-reducing-the-minimum-load-of-fossil-fired-plants/>

[47] N.-P. Yu, C.-C. Liu, and J. Price, "Evaluation of market rules using a multi-agent system method," *IEEE Transactions on Power Systems*, vol. 25, no. 1, pp. 470–479, 2010.

[48] J. D. Wojcik and J. Wang, "Feasibility study of combined cycle gas turbine (ccgt) power plant integration with adiabatic compressed air energy storage (acaes)," *Applied Energy*, vol. 221, pp. 477–489, 2018.

[49] F. J. Brooks, "Ge gas turbine performance characteristics," GE Power Systems, Tech. Rep., 2000.

[50] O. Anderson, M. A. Bragin, and N. Yu, "Optimizing deep decarbonization pathways in California with power system planning using surrogate level-based Lagrangian relaxation," *Applied Energy*, vol. 377, 2025.

[51] NVIDIA, "Nvidia a100 tensor core gpu architecture," <https://images.nvidia.com/aem-dam/en-zz/Solutions/data-center/nvidia-ampere-architecture-whitepaper.pdf>, 2020.

[52] ——, "Nvidia h100 tensor core gpu architecture," <https://www.advancedclustering.com/wp-content/uploads/2022/03/gtc22-whitepaper-hopper.pdf>, 2022.

[53] ——, "Nvidia blackwell architecture technical brief," https://cdn.prod.website-files.com/61ddda2012f29b7fc52c5fbaf6602ea9d0ce8cb73fb6de87f_nvidia-blackwell-architecture-technical-brief.pdf, 2024.

[54] R. N. Calheiros, E. Masoumi, R. Ranjan, and R. Buyya, "Workload prediction using arima model and its impact on cloud applications' qos," *IEEE Transactions on Cloud Computing*, vol. 3, no. 4, pp. 449–458, 2015.

[55] K. Cetinski and M. B. Juric, "Ame-wpc: Advanced model for efficient workload prediction in the cloud," *Journal of Network and Computer Applications*, vol. 55, pp. 191–201, 2015.

[56] S. Di, D. Kondo, and W. Cirne, "Host load prediction in a google compute cloud with a bayesian model," in *SC'12: Proceedings of the International Conference on High Performance Computing, Networking, Storage and Analysis*. IEEE, 2012, pp. 1–11.

[57] W. Fang, Z. Lu, J. Wu, and Z. Cao, "Rpps: A novel resource prediction and provisioning scheme in cloud data center," in *2012 IEEE Ninth International Conference on Services Computing*, 2012, pp. 609–616.

[58] C. Liu, C. Liu, Y. Shang, S. Chen, B. Cheng, and J. Chen, "An adaptive prediction approach based on workload pattern discrimination in the cloud," *Journal of Network and Computer Applications*, vol. 80, pp. 35–44, 2017.

[59] G. M. Wamba, Y. Li, A.-C. Orgerie, N. Beldiceanu, and J.-M. Menaud, "Cloud workload prediction and generation models," in *2017 29th International Symposium on Computer Architecture and High Performance Computing (SBAC-PAD)*, 2017, pp. 89–96.

[60] Q. Zhang, L. T. Yang, Z. Yan, Z. Chen, and P. Li, "An efficient deep learning model to predict cloud workload for industry informatics," *IEEE Transactions on Industrial Informatics*, vol. 14, no. 7, pp. 3170–3178, 2018.

[61] A. Jahanshahi, M. Rezvani, and D. Wong, "Wattwiser: Power & resource-efficient scheduling for multi-model multi-gpu inference servers," in *2023 IEEE 14th International Green and Sustainable Computing Conference (IGSC)*, 2023.

[62] NVIDIA, "Green contexts - cuda driver api," 2025, accessed: 2025-10-29. [Online]. Available: https://docs.nvidia.com/cuda/cuda-driver-api/group__CUDA__GREEN__CONTEXTS.html

[63] J. Bakits and J. H. Anderson, "Hardware compute partitioning on nvidia gpus for composable systems," in *37th Euromicro Conference on Real-Time Systems (ECRTS 2025)*, 2025. [Online]. Available: <https://drops.dagstuhl.de/entities/document/10.4230/LIPIcs.ERCTS.2025.21>

[64] Q. Weng, L. Yang, Y. Yu, W. Wang, X. Tang, G. Yang, and L. Zhang, "Beware of fragmentation: Scheduling {GPU-Sharing} workloads with fragmentation gradient descent," in *2023 USENIX Annual Technical Conference (USENIX ATC 23)*, 2023, pp. 995–1008.

[65] L. De Moura and N. Bjørner, "Z3: An efficient smt solver," in *International conference on Tools and Algorithms for the Construction and Analysis of Systems*. Springer, 2008, pp. 337–340.

[66] AMD, "Rocm system management interface (rocm smi) library," <https://github.com/ROCM/ROCM-smi>, 2024.

[67] A. Jahanshahi, M. Chow, and D. Wong, "Scaleserve: A scalable multi-gpu machine learning inference system and benchmarking suite," in *Proceedings of the 14th Workshop on General Purpose Processing Using GPU*, 2022, pp. 1–2.

[68] C. Chou, L. N. Bhuyan, and D. Wong, "μDPM: Dynamic power management for the microsecond era," in *2019 IEEE International Symposium on High Performance Computer Architecture (HPCA)*, Feb. 2019, pp. 120–132.

[69] X. Yang, S. M. Blackburn, and K. S. McKinley, "Elfen scheduling: Fine-grain principled borrowing from latency-critical workloads using simultaneous multi-threading," in *2016 USENIX Annual Technical Conference (USENIX ATC 16)*, Jun. 2016.

[70] A. Radford, J. Wu, R. Child, D. Luan, D. Amodei, I. Sutskever *et al.*, "Language models are unsupervised multitask learners," *OpenAI blog*, vol. 1, no. 8, p. 9, 2019.

[71] SWIMProjectUCB, "Swim project," 2013. [Online]. Available: <https://github.com/SWIMProjectUCB/SWIM/wiki>

[72] M. Świerniński, D. I. Stroe, R. Lærke, A. I. Stan, P. C. Kjær, R. Teodorescu, and S. K. Kær, "Field Experience from Li-Ion BESS Delivering Primary Frequency Regulation in the Danish Energy Market," *ECS Transactions*, vol. 61, no. 37, Sep. 2014.

[73] J. Hamilton, "Overall data center costs," 2025. [Online]. Available: <https://perspectives.mvdirona.com/2010/09/overall-data-center-costs/>

[74] L. A. Barroso, J. Clidaras, and U. Hölzle, *The Datacenter as a Computer: An Introduction to the Design of Warehouse-Scale Machines, Second Edition*, 2013.

[75] Google, "Google data center pue performance," 2025. [Online]. Available: <https://datacenters.google/efficiency/>

[76] E. Corporation, "Amd instinct mi300 series systems," 2025. [Online]. Available: <https://www.exactxcorp.com/category/AMD-Radeon-Instinct-Solutions>

[77] CAISO, "Market performance report, april 2024, ifm procurement and prices," 2025. [Online]. Available: <https://www.caiso.com/content/monthly-market-performance/apr-2024/ancillary-services.html>

[78] W. Wang, A. Abdolrashidi, N. Yu, and D. Wong, "Frequency regulation service provision in data center with computational flexibility," *Applied Energy*, vol. 251, p. 113304, 2019.

[79] C. Li, R. Wang, T. Li, D. Qian, and J. Yuan, "Managing green datacenters powered by hybrid renewable energy systems," in *11th International Conference on Autonomic Computing (ICAC 14)*, Jun. 2014, pp. 261–272.

[80] S. Govindan, A. Sivasubramanian, and B. Urgaonkar, "Benefits and limitations of tapping into stored energy for datacenters," in *2011 38th Annual International Symposium on Computer Architecture (ISCA)*, June 2011, pp. 341–351.

[81] R. Cochran, C. Hankendi, A. K. Coskun, and S. Reda, "Pack & cap: adaptive dvfs and thread packing under power caps," in *Proceedings of the 44th Annual IEEE/ACM International Symposium on Microarchitecture*, ser. MICRO-44, 2011.

[82] S. Wu, Y. Chen, X. Wang, H. Jin, F. Liu, H. Chen, and C. Yan, "Precise Power Capping for Latency-Sensitive Applications in Datacenter," *IEEE Transactions on Sustainable Computing*, pp. 1–1, 2018.

[83] R. Cochran, C. Hankendi, A. K. Coskun, and S. Reda, "Pack & cap: Adaptive DVFS and thread packing under power caps," in *44th Annual IEEE/ACM International Symposium on Microarchitecture*, 2011.

[84] M. Chow, K. Ranganath, R. Lerials, M. S. Carolan, and D. Wong, "Energy efficient task graph execution using compute unit masking in gpus," in *Redefining Scalability for Diversely Heterogeneous Architectures Workshop (RSDHA)*, 2021.

[85] C.-H. Hsu, Q. Deng, J. Mars, and L. Tang, "SmoothOperator: Reducing Power Fragmentation and Improving Power Utilization in Large-scale Datacenters," in *23rd International Conference on Architectural Support for Programming Languages and Operating Systems*, 2018.

[86] A. Jahanshahi, H. Z. Sabzi, C. Lau, and D. Wong, "Gpu-nest: Characterizing energy efficiency of multi-gpu inference servers," *IEEE Computer Architecture Letters*, vol. 19, no. 2, pp. 139–142, 2020.

[87] K. Ranganath, J. D. Suetterlein, J. B. Manzano, S. L. Song, and D. Wong, "Mapa: Multi-accelerator pattern allocation policy for multi-tenant gpu servers," in *Proceedings of the International Conference for High Performance Computing, Networking, Storage and Analysis*, 2021, pp. 1–14.